

Signature Analysis for Channel and Source Authentication in Optical Networks

STAMATIOS V. KARTALOPOULOS, PhD
Williams Professor in Telecommunications Networking
ECE Department/TCOM Graduate Program in Optical Networking
The University of Oklahoma
4502 E. 41st Street, Tulsa, OK 74135
USA

Abstract: - Network security has traditionally been limited to network access and network administration, whereas data security is left to end clients where text is encrypted and decrypted. In the last decade, there has been a rapid increase in bandwidth demand mainly due to the explosion of the Internet and mobile telephony. The explosive bandwidth has been comfortably met with optical networks having many optical channels multiplexed in the same fiber, known as wavelength division multiplexing. Data rate exceeding 1 Tbps within a fiber implies that there are tributaries that carry sensitive and proprietary data. Although data are encrypted by the end client, there is no assurance that, if captured by an eavesdropper, they may not be decrypted. Therefore, three new requirements emerge; monitor the optical link integrity, detect if an optical channel is compromised by tapping the fiber, and adopt a countermeasure strategy. One way to accomplish this is to monitor the channel performance parameters for changes in real-time. In this paper, we analyze key performance parameters of the optical signal, we describe how these parameters impact the channel performance. In addition, we develop a method to estimate in real-time the bit error rate and signal to noise ratio, and how these can be used to detect fiber intrusion. Finally, we develop a countermeasure protocol that we believe outsmarts the eavesdropper.

Keywords: - Optical networks security, Communications security, Intrusion detection

1 Introduction

Securing information with cryptographic and encoding methods has been practiced since antiquity. The term “cryptography” and “steganography” are compound words derived from ancient Greek.

In modern communications, securing data from unauthorized intruders is left to the responsibility of end users who use encryption algorithms. However, based on recent events, even aggressive encryption algorithms have been broken. Currently, the network assures that its nodes are provisioned correctly and that data are protected from network failures but they are not secured from intruders; traditionally, network security has been limited to network access for provisioning and administration.

During the last decade, we witnessed a rapid increase of bandwidth demand mainly due to the explosion of the Internet and mobile telephony. This explosive bandwidth has been comfortably met with optical networks and particularly with an

optical technology known as wavelength division multiplexing (WDM) by which many optical channels are multiplexed within the same fiber. Currently, the aggregate data rate per single fiber has exceeded 1 Tbps. Such data rate within a fiber implies that there are tributaries with sensitive, proprietary and secret data. Thus, although data are encrypted by the end user, there is no assurance that they are immune to an eavesdropper who may access them and decipher them. Therefore, in addition to data, the network itself, as the transportation vehicle is required to protect the data that transports, encrypted or not. In such case, three new requirements emerge: monitor the optical link integrity, detect when a channel is compromised by fiber tapping, and include a countermeasure strategy to outsmart the eavesdropper in order to continue uninterrupted reliable and secure service. To accomplish this, the performance of link parameters must be understood and the transfer function of each channel must be continuously

monitored; we call this signature analysis and monitoring.

Link and channel signature analysis starts with quantifying a number of parameters from the transmitter up to including the receiver such as optical power, wavelength grid, channel separation, and fiber and link component parameters. Based on these, the linear and non-linear photon-matter interactions are calculated and to what degree the channel performance is degraded and if failures may be caused [1, 2]. At the receiver, channel performance parameters are used to deduct whether gradual changes are caused by natural degradations or whether step-wise changes are caused by intervention or faults.

In this paper, we analyze key performance parameters of the optical signal as constituents of the channel signature, and we describe how variability of these parameters impact the channel signature. In addition, we develop a method to estimate in real-time the bit error rate, Q-factor and signal to noise ratio, and how these can be used to detect fiber intrusion. Finally, we develop a countermeasure protocol that we believe outsmarts the eavesdropper.

2 Parameters that influence the optical signal quality

The parameters that influence the optical signal are classified in linear and non-linear. In addition to this, there is a vertical classification in time-dependent parameters.

2.1 Time-dependent parameters

Time-dependent parameters are jitter of the modulated signal, temporal fluctuation of signal spectral density, temporal fluctuation of signal optical power, and temporal fluctuation of signal polarization of state

Laser chirp and optical amplifiers are the main contributors of jitter. Jitter degrades the received signal, it narrows the sampling window at the receiver, and it is manifested by lateral eye diagram closure, Figure 1. For example, laser chirp under large signal stimulation is expressed by [3] $2\pi\Delta f(t) = \alpha/2 [dP/2dt + 2\pi K_P P - 2\pi K_{SP}/P]$, where α is the linewidth enhancement factor, P is the laser output power, K_P and K_{SP} are the contributions of non-

linear suppression and of spontaneous emission to adiabatic chirp.

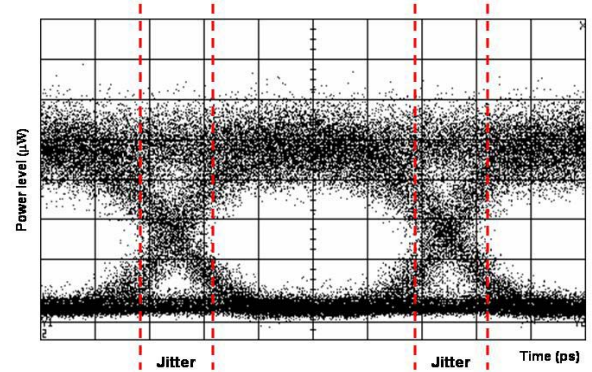


Figure 1. Eye diagram at the receiver with jitter

Temporal fluctuation of spectral density is caused by laser drift and optical amplifiers. In addition, the signal below the zero-dispersion point causes temporal broadening of the pulse. Temperature, pressure, filter stability, and other conditions may also cause drift of the operating frequency. Variations of spectral density impact chromatic dispersion, channel spacing, and other parameters. These variations impact the standard deviation of spectral distribution and the power level of the received signal. The frequency deviation is then calculated from $\Delta f(t) = -(c/\lambda_{\text{mean}}^2)[\lambda(t) - \lambda_{\text{mean}}]$, where λ_{mean} is the mean wavelength of the laser source.

Temporal fluctuation of optical power is caused by lasers and other components, including channel re-assignment and channel add-drop. Power fluctuation impacts the signal to noise ratio and bit error rate.

Some temporal fluctuations are also attributed to ambient temperature variations, which affect the signal propagation (group velocity) and polarization state in fiber.

2.2 Linear and non-linear parameters

Linear or non-linear interactions between matter and photons stem from the refractive index of matter. The refractive index of fiber has a transfer characteristic that consists of a linear and a non-linear region, $n = n_0 + a_1 E^1 + a_2 E^2 + \dots$

Isotropic matter behaves linearly when it is free of stress (thermal, mechanical or optical), and if the optical signal through it has low power. The linear behavior of matter causes phase shift of the propagating optical wave that through it, group velocity dispersion (GVD) as a result of phase shift

variability between frequencies, dispersion as a result of speed variability between frequencies, and spontaneous noise (optical amplifiers)

Matter with non-symmetrical crystalline structure or under the influence of stress or high optical power interacts non-linearly with light. This causes four wave mixing (FWM), self-phase modulation (SPM), cross-phase modulation (XPM), stimulated Brillouin scattering (SBS), stimulated Raman scattering (SRS), chromatic dispersion slope (S), polarization mode dispersion (PMD), and polarization dependent loss (PDL).

2.2.1 Attenuation

Attenuation is the effect of scattering and/or absorption of photons by impurities or by disturbances in the uniform matrix of matter. In addition, the optical signal loses power by connectors, splices and other components [4]. If the input and optical power at the entry and exit point of a 1 km long fiber is P_{in} and P_{out} (measured in mW), respectively, the optical attenuation over a fiber span L , L_{span} , is $L_{span} = \alpha L = 10 \log_{10}[P_{out}/P_{in}]$ (in dB), where α is the optical power attenuation coefficient.

Power loss (in dB) is additive and thus the total power is a straightforward algebraic summation. The total loss in a path is calculated by the summation $P_e - \Sigma L_n - \Sigma L_s - \Sigma L_c - \Sigma L_{N-L} - \Sigma L_{N-N} + \Sigma G_n$, where P_e is the power launched in the fiber, L_n the power loss of each fiber segment, L_s the mean splice loss, L_c the mean loss of line connectors, ΣL_{N-L} the sum of power degradations due to non-linear effects, ΣL_{N-N} the sum of noise sources such as ASE, and ΣG_n the sum of amplifier gain (if applicable).

2.2.3 Amplifier Gain

Amplification overcomes signal attenuation. Currently, there are erbium doped fiber amplifiers (EDFA), Raman, and semiconductor optical amplifiers (SOA). Each of them has distinct gain profiles and spectral utilization. At first approximation, amplifier gain is considered flat over the spectral range of amplification; this is an ideal case that assumes perfect *gain flattened filters* at the output of the amplifier. In reality, the signal power has a standard deviation σ measured at the output filter; for M cascaded amplifiers, the total

standard deviation, or variance is $\sigma_{tot}^2 = \Sigma \sigma_k^2$, for $k=1$ to M

2.2.4 Raman Gain, ASE and Noise Figure

The unsaturated Raman gain is expressed as $G_R = I_{out}/I_{in} = \exp[RPL_{eff}/A_{eff}] \exp[-\alpha_s L]$, where A_{eff} is the effective area of the fiber core and L_{eff} is the length of fiber for which Raman is effective, R is the Raman coefficient, P is the pump power, α_s is the fiber attenuation coefficient at the wavelength of the signal and L the fiber length.

Although amplifier spontaneous emission (ASE) is unavoidable, RAMAN ASE is less than EDFA ASE. The noise transfer from Raman pump to signal for a co-propagating pump is $R_s \sim R_p + 20 \log(\ln G_R) + 10 \log[(v_s/L_{eff})^2 / \{(\alpha_p v_s)^2 + (2\pi D \Delta \lambda \cdot v_s f)^2\}]$, and for counter-propagating pump it is $R_s \sim R_p + 20 \log(\ln G_R) + 10 \log[(v_s/L_{eff})^2 / \{(\alpha_s v_s)^2 + (2\pi f)^2\}]$, where the parameter α_p and α_s are the attenuation coefficients at the pump and signal wavelengths, v_s is the velocity of signal in the fiber, D is the chromatic dispersion, and $\Delta \lambda$ is the wavelength difference between pump and signal.

The noise figure is a measure of added noise to the signal. Thus, an equivalent noise figure is defined as $NF_R = [(R_{ASE}/h\nu) + 1] / G_R$, where R_{ASE} is the Raman ASE density at the end of the fiber, G_R is the ON/OFF Raman gain, h is Plank's constant and ν is the optical frequency.

The Raman pump power is strong compared with the signal. Due to non-linear phenomena stimulated by the Raman pump, noise is added to the optical signal. If the fiber span loss is L_f , then the noise figure for the span (without pump) is defined as $NF_{unpumped} = 1 / L_f$. Then, the noise figure for the Raman pumped fiber span is modified to $NF_R = [P_{noise}/(h\nu \Delta \nu G_R L_f)] + 1 / (G_R L_f)$ (in dB), where P_{noise} is the noise power in the electrical filter bandwidth (here we assume that the signal has been received and converted to electrical), and G_R is the Raman gain. Based on the two noise figures, an improvement noise figure is calculated from $NF_{improvement} = NF_R - NF_{unpumped}$ (dB).

Because of the Raman non-flat gain, Raman amplification induces a signal power tilt; a power increase in shorter-wavelengths within its amplification range and a power decrease in longer-wavelengths. The SRS induced overall power tilt, ΔP , is expressed by $\Delta P = -10 \log[1 - \eta_{pol} \{G_R \Delta f P_{ch} L_{eff} N(N-1) / 2 A_{eff} \Delta f_R\}]$, where h_{pol} is a factor of co-polarization of the DWDM channels (for fully copolarized it is 2 and for non-copolarized it is 1), Δf

is the channel spacing, P_{ch} is the power per channel, and N is the number of channels.

For each fiber link, a figure of merit (FOM) is defined as a function of the effective length of Raman, $L_{eff} = n_R/\alpha$, where n_R is the refractive index at the Raman wavelength, $A_{eff-pump}$ the effective area of the fiber at the pump wavelength, and G_R , $FOM = L_{eff} A_{eff-pump} / G_R$ the Raman gain coefficient.

In practice, several Raman-pumps, each at different frequency, are required to amplify a wide spectral range. In this case, the above relationships become more complex and a gain ripple effect needs to be considered with an average variation between 0.1 and 0.5 dB

In addition, a penalty in Q-factor is defined, expressed as Penalty (dB) = $10\log\{\sqrt{1 + Q^2\int(R_N(f)df)}\}$, where the integral is from f_1 to f_2 , and R_N is the Raman noise transfer from pump to signal (in dB/Hz).

2.2.5 EDFA Gain, ASE and Noise figure

The extended range EDFA provides gain in both the C and L-bands. If the small signal power gain is G_0 , the EDFA gain is $G = G_0/(1+\beta G_0)$, where β is the ratio of the total average power in the fiber over the saturation output power.

The ASE noise strength by the EDFA is approximated as $N_{ASE} = aG_{EDFA}h\nu B$, where a is a constant between 1 and 2, G_{EDFA} is the EDFA average gain, and B is the bandwidth [5]. If N_{ASE} represents ASE in one polarization state at the EDFA output, then the noise figure for the EDFA is $NF_{ASE} = [(1/G_{EDFA})\{(2N_{ASE}/h\nu B)+1\}]$. Substituting N_{ASE} in the latter yields $NF_{ASE} = (2\alpha G_{EDFA} + 1)/G_{EDFA}$.

Since noise is cumulative, the noise figure over a path with N EDFAs is the sum, $NF_{N,Total} = 10\log_{10} [NF_1 + (NF_2-1)/G_1 + (NF_2-1)/G_1G_2 + (NF_3-1)/G_1G_2G_3 + \dots]$ (dB)

The SNR at the receiver, based on ASE noise, is approximated to $SNR_{rec} (dB) = 58(dB) + P_{in} (dBm) - NF_{N,Total} (dB)$

2.3 Crosstalk

In DWDM, adjacent channels interact and optical power is transferred from one to the other through photon-matter-photon interaction. This transfer causes crosstalk manifested as noise on the signal [6]. Since noise is cumulative, assuming that the crosstalk-noise to signal ratio (CSR) of adjacent

channels is δ_k , the CNR for N links is δ_{tot} , is $\delta_{tot} = \sum\delta_k$.

Crosstalk degrades the quality of the received signal, which is manifested by eye closure, the penalty of which, $P_{crosstalk}$, is estimated as $P_{crosstalk} = -5\log_{10} [1-2\sqrt{\delta_{tot}}]$.

2.4 Chromatic dispersion

If the fiber chromatic dispersion coefficient and the slope coefficient at a wavelength λ_0 is D_0 (measured in ps/nm-km) and S_0 (measured in ps/nm²-km), respectively, then the chromatic dispersion coefficient at a wavelength λ is [7, 8], $D(\lambda) = D_0 + (\lambda - \lambda_0)S_0$. Then, the pulse spread $\Delta\tau$ (in ps) due to chromatic dispersion is $\Delta\tau = \sigma = |D(\lambda)|L\Delta\lambda$, where $\Delta\lambda$ is the optical spectral width of the signal (in nm units).

Pulse spreading causes intersymbol interference (ISI), SNR decrease, and BER increase. As a consequence, dispersion bounds the bit rate achievable in a single optical channel by [9] $B^2DL < 10^5$.

2.5 Polarization Mode Dispersion

PMD is caused by fiber core birefringence and channel non-monochromaticity. Two orthogonally polarized states propagate with different group velocity causing polarization mode dispersion (measured in ps). The group delay (in ps) is expressed by [10] $\tau(\lambda) = \tau_0 + (S_0/2)\{\lambda - \lambda_0\}^2$.

The mean differential group delay (DGD) is a function of the fiber birefringence factor, which is a function of the optical frequency and of the fiber length [11]. In general, DGD is measured by the average difference of time arrival, $\Delta\tau$, between the two orthogonally polarized modes $\Delta\tau = (\Delta n_g L)/c$, where c is the speed of light, L is the length of the fiber and Δn_g is the refractive index variation corresponding to the group velocity of the orthogonal polarization states. If we ignore high-order frequency effects, and if D_{PMD} (measured in ps/(km)^{1/2}) is the average PMD fiber coefficient, then the DGD is expressed as $\Delta\tau_{PMD}^2 = D_{PMD}^2 L$.

PMD is cumulative. Therefore, if a path consists of M links, and assuming that there is no PMD compensation over the path, then the total DGD for the path is the square root of the sum of the squares of DGDs for each link $\Delta\tau_{PMD, TOT} = \sqrt{\sum(D_{PMD,k}^2 L_k^2)}$, over all M links.

As the two orthogonal polarization states propagate in the fiber-core there is variability in speed

due to non-uniform fluctuation of imperfections, known as *Stokes noise*, and due to optical channel wavelength content, known as *chromatic jitter*. In this case, the square of the relative DGD noise $[d(\Delta\tau)/\Delta\tau]$ is the sum of squares of each noise component (the Stokes-related and the jitter-related) $[d(\Delta\tau)/\Delta\tau]^2 = [d(\Delta S)/\Delta S]^2 + [d(\Delta\omega)/\Delta\omega]^2$, where $\Delta\omega$ is the spectral width, d is the differential operator and ΔS is the polarization state variability at the output of the fiber; the inverse of the latter is the “bandwidth efficiency factor”, $\alpha_B = 1/d(\Delta S)$. The bandwidth efficiency factor is characteristic of the measuring method (it may have a value from under 1 to more than 200) and it is related to signal to noise ratio (SNR) of the optical signal in the following sense $\text{SNR} \propto \alpha_B \Delta\tau \Delta\omega$. Thus, given the value of α_B , and measuring $\Delta\tau$ and $\Delta\omega$, the potential maximum SNR is calculated, and from this, the potential amount of noise.

2.6 Spectral broadening

The refractive index of many materials depends on the amplitude of the electrical field. Thus, as the electrical field changes so does the refractive index. Therefore, as an almost monochromatic light-pulse travels in a transparent medium, its amplitude variation causes *phase change* and *spectral broadening*.

The *phase change* is given by $\Delta\Phi = [2\pi(\Delta n)L]/\lambda$, where L is the fiber length, and Δn is the refractive index variation about the wavelength λ , $\Delta n = n(\lambda, E) - n_1(\lambda)$.

Phase variations are equivalent to frequency modulation or “chirping”. The *spectral broadening* is given by $\delta\omega = -d(\Delta\Phi)/dt$.

For a *Gaussian* shaped pulse, spectral broadening is $\delta\omega = 0.86\Delta\omega\Delta\Phi_m$, where $\Delta\omega$ is the spectral width and $\Delta\Phi_m$ is the maximum phase shift in radians.

Spectral broadening appears as if one half of the pulse is frequency downshifted (known as *red shift*) and the other half upshifted (known as *blue shift*).

2.7 Self-phase modulation

The dynamic characteristics of a propagating optical pulse in fiber, due to the Kerr effect of the medium, result in modulation of its own phase known as *self-phase modulation*. This non-linear phenomenon causes spectral broadening.

If the wavelength of the pulse is below the zero-dispersion point (known as *normal dispersion regime*), then spectral broadening causes temporal broadening of the pulse as it propagates. If the wavelength is above the zero-dispersion wavelength of the fiber (the *anomalous dispersion regime*) then chromatic dispersion compensates self-phase modulation and it reduces temporal broadening. In DWDM communications, this is one of the reasons to favor a small positive dispersion and not zero.

2.8 Self-modulation or modulation instability

When a single pulse of almost monochromatic light has a wavelength well above the zero-dispersion wavelength of the fiber (or the anomalous dispersion regime) another phenomenon occurs that further degrades the width of the pulse. That is, two side lobes are symmetrically generated at either side of the pulse, deforming the original pulse shape of the signal. This is known as *self-modulation* or *modulation instability*.

Modulation instability depends on material dispersion, on signal wavelength and its spectral density distribution, fiber length, and optical signal power. Modulation instability is considered a special four wave mixing case that affects the signal-to-noise ratio. It is reduced by operating at low power levels and/or at wavelengths below the zero-dispersion wavelength.

2.9 Four Wave Mixing

When three lightwave frequencies, f_1 , f_2 , and f_3 are closely spaced (in terms of wavelength), then, because of non-linear interactions of photon-matter-photon, a fourth lightwave frequency is generated, f_{fwm} . This is known as *four-wave mixing* (FWM), or *four-photon mixing*.

If the electric field of the three generating components are E_1 , E_2 , and E_3 , the refractive index is n , the non-linear refractive index is χ and the fiber loss is α , then the created component is E_{FWM} with angular frequency ω at the output of a fiber segment, L is described by $E_{FWM} = j [(2\pi\omega)/nc] d\chi E_1 E_2 E_3 e^{-\alpha(L/2)} \mathcal{F}(\alpha, L, \Delta\beta)$, where $\mathcal{F}(\alpha, L, \Delta\beta)$ is a function of fiber loss, fiber length and phase mismatch related to channel spacing and dispersion. In fact, at the zero-dispersion wavelength, FWM is at its best performance. Thus, as opposed to Raman scattering, four-wave mixing requires strong phase matching of coincident energy from all three wavelengths. As

such, chromatic dispersion and length of fiber reduce the intensity of the FWM product.

4 Bit error rate

4.1 Photodetector responsivity and noise contributors

The gain-current responsivity of a photodetector is given by $R = \eta eG/h\nu = \lambda \eta eG/hc$, where η is the quantum efficiency, e is the charge of the electron (1.6×10^{-19} C), G is the gain of the detector, h is Planck's constant, $\nu = c/\lambda$ is the optical frequency and c is the speed of light in free space (3×10^8 m/s).

The photodetector at the receiving end of the fiber converts the photonic signal with an efficiency that depends on its responsivity. The receiver itself adds its own share of noise, which consists of three contributors: dark current (N_{dark}), shot noise (N_{shot}) and Johnson noise (N_J), expressed by [16], $N_{\text{dark}} = 2e i_d B$, $N_{\text{shot}} = 2\eta e^2 P_{\text{diff}} B/h\nu$, and $N_J = 4kTB/R_L$, where B is the receiver bandwidth, k is the Boltzman constant, T is the ambient temperature, i_d is the photodetector dark current, and R_L is the output load across which the voltage is measured.

Now, the variance of the noise current per bit at the output of the receiver is $\sigma_{N_{\text{photon}}}^2 = 2(\eta P_R/h\nu)^2 \sigma_T^2$, where P_R is the incident photonic power per bit, and σ_T is the variance due to all contributing photonic and electronic noise variances, $\sigma_T^2 = \sum \sigma_i^2$.

The contributing photonic and electronic noise variances, σ_i^2 , receiver, dark current, optical amplifier ASE noise, filter, and relative intensity noise, are [17], $\sigma_{\text{RCVR}}^2 = 4kTB/R_L$, $\sigma_{\text{dark}}^2 = 2e i_d B$, $\sigma_{\text{ampl}}^2 = 4R^2 P_R \rho_{\text{ASE}} B$, $\sigma_{\text{filter}}^2 = 4gR^2 \rho_{\text{ASE}}^2 B^2$ and $\sigma_{\text{RIN}}^2 = i_d^2 n_{\text{RIN}} B$, where ρ_{ASE} is the spectral density of optical amplifier ASE, g is the ratio $\Delta\nu/B$, where $\Delta\nu$ is the optical filter bandwidth and B is the receiver bandwidth, and n_{RIN} is the relative intensity noise (RIN) factor.

When RIN is assumed white and Gaussian with a two-sided spectral density, the RIN spectral power density is expressed (in Hz) $\text{psd}_{\text{RIN}} = 0.5 \times 10^{(RIN/10)} P_{\text{Trans}}^2$, where RIN is the relative intensity noise parameter of the laser (measured in dB/Hz), and P_{Trans} is the average transmitted power.

Based on the above, the SNR is the ratio of the mean square value of the generated current by the

receiver to the total noise variance in the photocurrent. In this case, the target SNR based on the minimum power and minimum number of photons required to detect a one bit (of a bit period τ_c) may be approximated by $\text{SNR} = (\eta P_R/h\nu)^2 / [(e^2 \eta P_R/h\nu + e i_d + 2kT/R_L)B + (e\eta P_R/h\nu)^2 \sigma_{N_{\text{ph}}}^2 + (e\eta P_R/h\nu)^2 \tau_c B]$.

Finally, if the receiver has a transimpedance amplifier (TIA), then the power spectral density of the TIA input noise is $\text{psd}_{\text{TIA}} = (I_n/R)^2/2n_{\text{TIA}}$, where I_n is the input referred noise current of the TIA, the factor 2 appears because of the two sided spectral density, and n_{TIA} is the noise bandwidth of the TIA defined as $n_{\text{TIA}} = (1/2\pi) \int_0^\infty |F_o(\omega)|^2 d\omega$, where the integral is from 0 to infinity.

4.2 Probability of errored bits

A bit in error is a random process and its mathematical treatment is based on stochastic processes and probabilities. In communications, the ratio of detected erroneous bits, ϵ , to total bits transmitted, n , is expressed as $P(\epsilon)$ [18] $P(\epsilon) = \epsilon/n$.

In communications, the estimated probability $P'(\epsilon)$ for a large sample of bits is almost equal to the actual value. Typically, an upper limit of $P'(\epsilon)$ is set to a specified level γ , such as $\gamma = 10^{-N}$, where N depends on application and it may vary from 8 to 15. To estimate an acceptable error probability, one resorts to statistical methods and binomial distribution functions. Thus, if p is the probability that a bit will be in error, and q is the probability that a bit will be correct, then the probability that k bit errors will occur in n transmitted bits is expressed by $P_n(k) = \{n!/(k!(n-k)!)\} p^k q^{n-k}$.

Similarly, the probability that N or fewer errors will occur in n transmitted bits is expressed by $P(\epsilon \leq N) = \sum P_n(k) = \sum [\{n!/(k!(n-k)!)\} p^k q^{n-k}]$, where the sum is calculated from $k=0$ to N , and in the case of N or more errors, $P(\epsilon > N) = 1 - P(\epsilon \leq N) = \sum P_n(k) = \sum [\{n!/(k!(n-k)!)\} p^k q^{n-k}]$, where the sum is calculated from $k=N+1$ to n .

The above equations are simplified if errors are considered to be Poisson random. In this case and for n very larg, $p^k q^{n-k} = \{(np)^k/k!\} e^{-np}$, and thus $\sum P_n(k) = \sum \{(np)^k/k!\} e^{-np}$.

The probability that the actual $P(\epsilon)$ is better than the acceptable set level γ , is known as the confidence level, CL, expressed in percent (%) and defined as $\text{CL} = P(\epsilon > N|\gamma) = 1 - \sum [\{n!/(k!(n-k)!)\} P^k (1-\gamma)^{n-k}]$, where the sum is calculated from $k=0$ to N . The last equation can be solved for n , the number of transmitted bits

required to be monitored for errors. Clearly, the number n in the unit of time is directly related to the bit rate. Assuming a confidence level of 99%, a BER threshold set at $\gamma=10^{-10}$, and a bit rate of 2.5 Gbps, then the required number n is 6.64×10^{10} to detect a single error.

5 BER and eye-diagram

In transmission, a quick and qualitative measure of the signal quality is the “eye-diagram”. Based on the characteristics of the eye diagram, a real-time estimation method has been developed that determines the signal performance parameters BER, SNR, Q-factor, power level, and more [xx]. This method has served to define a digital circuit that estimates without signal disruption and in real time the signature of the incoming signal. In addition, the circuit has the ability to track performance changes; slow changes are analyzed to identify degradations and fast or abrupt changes to identify faults or intrusion by an eavesdropper, Figure 2.

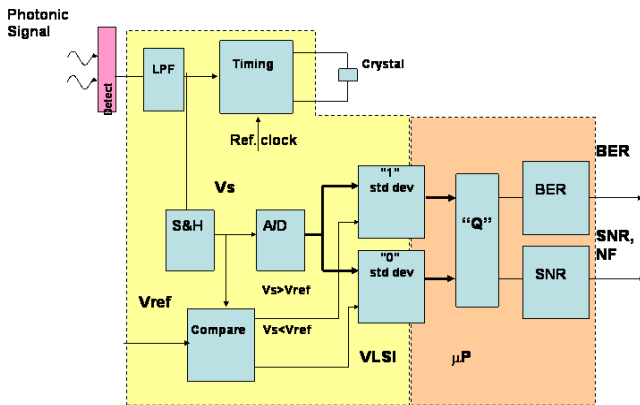


Figure 2: Circuitry for the estimation of BER, Q-factor and SNR and signature analysis.

6 Countermeasures

The analyzed signal signature infers whether a channel is degrading or an eavesdropper has intervened. If degradations are severe, they are reported with a control message and a remedial action is invoked. However, if changes emulate those of an eavesdropper, then the receiver alerts the transmitter with a control message over a separate path and channel, in a closed loop

configuration. In this case, the transmitter continues transmitting (encrypted but unclassified) messages over the eavesdropped channel, and the encrypted and classified messages over a reassigned DWDM channel, Figure 3.

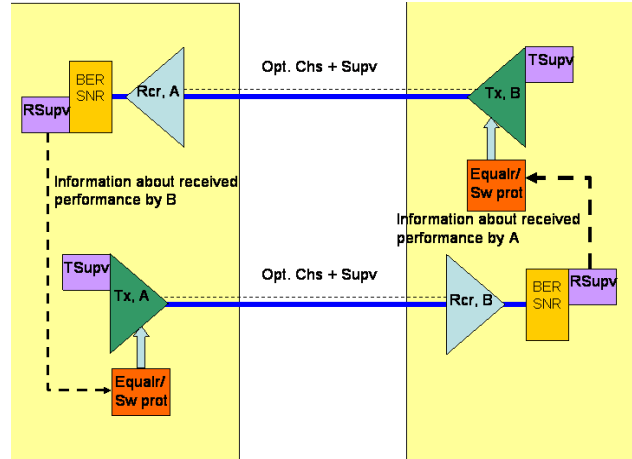


Figure 3: A closed loop model of an optical link for the reassignment of channel.

The control messages follow a protocol, Figure 4. Here, “NO DIFF” indicates no channel signature, and “CHNL REASSIGN RQST” indicates a request for channel reassignment. In this case, the transmitter searches for another channel from a pool of reserved ones and it responds with a wavelength (re)assignment control message (λ -REASSIGN”), while it moves encrypted classified traffic from the intercepted channel to the newly assigned wavelength. The receiving end selects the newly assigned wavelength and it starts monitoring its performance and signature. If after the reassignment, the change continues, then the receiver sends another “CHNL REASSIGN RQST”, and so on. If after an exhaustive reassignment the problem persists, then a link failure is declared by both the transmitting and receiving ends and another fiber is searched for. Conversely, if the transmitting end does not find an available channel, then a “NO λ PROT AVAIL” control message is sent to the receiver, in which case another fiber is searched for, while unclassified service continues over the suspicious channel. This method is termed *channel proactive reassignment algorithm* (CPRA).

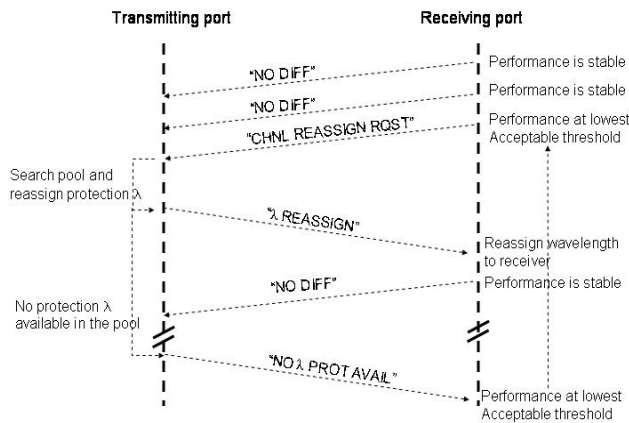


Figure 4: Protocol of the channel proactive reassignment algorithm.

7. Conclusion

The sustained performance of the optical link and optical path are of paramount importance in optical network security. A good link and path optical budget impacts directly the network design, topology, management and cost of service. Thus, an intervention on a good link will alter its characteristics and its signature, which in turn affect the performance parameters of the channel. Monitoring the performance parameters in real-time, malicious interventions are detected and a countermeasure strategy is followed.

In this paper, we presented a comprehensive analysis of parameters that affect the optical signal signature, as well as the related performance parameters. We also outlined a probabilistic method of errored bits and how the performance parameters are monitored with an integrated circuit that is based on eye diagram estimation method. We finally described countermeasure strategy, whereby the source is mimicking encrypted data (which however are unclassified) whereas encrypted classified data is transmitted over a reassigned channel.

References

[1] S.V. Kartalopoulos, "DWDM: Networks, Devices and Technology", IEEE Press/John Wiley Publ., 2003
 [2] S.V.Kartalopoulos, "Fault Detectability in DWDM", IEEE Press, 2001

[3] G.P. Agrawal and N.K. Dutta, "Long wavelength semiconductor lasers", John Wiley Publ., 1986
 [4] G.P. Agrawal, "Nonlinear Fiber Optics", Academic Press, San Diego, 1995.
 [5] E. Desurvire, "Erbium Doped Fiber Amplifiers", John Wiley Publ., New York, 1994
 [6] P.S. Andre, L.L. Pinto, A.N. Pinto, and T. Almeida, "Performance Degradations due to Crosstalk in Multiwavelength Optical Networks Using Optical Add Drop Multiplexers Based on Fibre Bragg Gratings", *Revista Do Detua*, Portugal, vol. 3, no. 2, Sept. 2000, pp. 85-90.
 [7] ITU-T Recommendation G.653, "Characteristics of a dispersion-shifted single-mode optical fibre cable", 1997.
 [8] S.V. Kartalopoulos, "Introduction to DWDM Technology: Data in a Rainbow", IEEE/Wiley, 2000.
 [9] A.R. Chraplyvy, "High-Capacity Lightwave Transmission Experiments", *Bell Labs Tech. J.*, vol. 4, no.1, 1999, 230-245
 [10] ITU-T Recommendation G.655, "Characteristics of a non-zero-dispersion shifted single-mode optical fibre cable", 1996.
 [11] ITU-T Recommendation G.650, "Definition and test methods for the relevant parameters of single-mode fibres", 1997.
 [12] C.E. Shannon, "A Mathematical Theory of Communication", *Bell System Tech. J.*, vol 27, pp. 379-423, 623-656, 1948.
 [13] P.P.Mitra and J.B. Stark, "Nonlinear limits to the information capacity of optical fibre communications, *Nature*, vol 411, pp. 1027-1030, 2001.
 [14] E. Narimanov, and P.P. Mitra, "The Channel Capacity of a Fiber Optics Communication System", *Proceeding of OFC 2002*, paper ThQ1, pp. 504-505, 2002.
 [15] H. Kogelnik, "High-capacity optical communications", *IEEE Sel. Topics Quant. Elec.* Vol. 6, no. 6, pp. 1279, 2000.
 [16] A. Yariv, "Optical Electronics", 3rd ed., Chapter 11, pp. 345-382, CBS College Publishing, New York, 1991/
 [17] G.P. Agrawal, "Fiber-Optic Communications Systems", Wiley, New York, 1992.

- [18] A. Papoulis, "Systems and Transforms with Applications in Optics", McGraw-Hill, New York, 1968
- [19] N. Hanik, et al., "Application of amplitude histograms to monitor performance of optical channels", *Electronic Letters*, vol. 5, pp. 403-404, 1999.
- [20] G. Bendelli, C. Cavazzoni, R. Giraldi, and R. Lano, "Optical Performance monitoring techniques", *Proceedings of ECOC 2000*, vol. 4, pp. 113-116, 2000.
- [21] C.M. Weinert, "Histogram method for performance monitoring of the optical channel", *Proceedings of ECOC 2000*, vol. 4, pp. 121-11622, 2000.
- [22] I. Shake, and H. Takara, "Transparent and Flexible Performance Monitoring Using Amplitude Histogram Method", *OFC'02 Tech. Digest*, paper TuE1, pg. 19-21, OFC'02, Anaheim, CA, 2002.